Wireless Personal Communications (2021) 121:1607–1625
https://doi.org/10.1007/s11277-021-08687-7

Non Orthogonal Multiple Access Using Reconfigurable Intelligent Surfaces

Ghassan Alnwaimi[1] · **Hatem Boujemaa**[2]

Accepted: 17 June 2021 / Published online: 1 July 2021

Abstract
In this paper, we propose the use of Reconfigurable Intelligent Surfaces (RIS) for Non Orthogonal Multiple Access (NOMA). RIS is decomposed in N sets of reflectors serving N users. The ith RIS contains N_i reflectors dedicated to user i. When RIS is used, all reflections reach the ith user with the same phase. RIS has not been yet used in NOMA systems where the transmitter sends a combination of symbols dedicated to N user. The ith user U_i has to detect the symbols of remaining $N-i$ users. It performs Successive Interference Cancelation and detects first the symbol of weakest user. Then, it removes the signal of weakest user and detect that of second weakest user. The process is continued until U_i detects its own symbol. We suggest to optimize power allocation coefficients to all users as well as the number of reflector dedicates to each user in order to maximize the total throughput using the alternating maximization algorithm. More power and a larger number of reflectors should be allocated to weak users. An example of RIS implementation is provided in Dai et al. (IEEE Access, 8:45913–45923, 2020).

Keywords Reconfigurable intelligent surfaces (RIS) · Non orthogonal multiple access (NOMA) · Optimal power allocation · Optimal number of reflectors · Rayleigh fading channels

1 Introduction

Reconfigurable Intelligent Surfaces (RIS) can be used in future 6G wireless communications to ensure higher data rates. When RIS is used as reflector, the received signal at destination can be viewed as the output of a Maximum Ratio Combiner (MRC) [2] resulting in larger Signal to Noise Ratio (SNR) than conventional wireless systems without RIS. RIS can be used as a reflector or a transmitter [2]. When RIS is used as reflector, the phase of ith reflecting meta-surface of RIS is optimized to compensate the phases of product of

✉ Ghassan Alnwaimi
galnwaimi@kau.edu.sa

Hatem Boujemaa
boujemaa.hatem@supcom.tn

1 King Abdulaziz University, Jeddah, Kingdom of Saudi Arabia

2 SUP'COM, Aryanah, Tunisia

channel gains between Base Station (BS)/RIS and RIS/destination [3]. All N reflections over RIS reach the destination with the same phase resulting in a high SNR [4–6]. RIS requires a perfect knowledge of channel phases of BS-RIS and RIS-Destination links [2]. When RIS is used as transmitter, RIS is illuminated with an antenna of Base Station (BS). The phase of kth reflector of RIS depends on the phase of channel gain between RIS and destination as well as the phase of transmitted Phase Shift Keying (PSK) symbol. RIS don't consume much power and are nearly passive [2]. A hardware architecture of RIS has been proposed in [7].

Throughput maximization for wireless communications using RIS has been proposed in [8]. Non Orthogonal Multiple Access (NOMA) using RIS has been discussed in [9] where N_1 and N_2 reflectors are dedicated to weak and strong users. In [9], the authors derived the bit and symbol error probabilities of NOMA using RIS. The source sends a combination of symbols dedicated to near and far users. The transmitted signal is reflected by RIS and forwarded to far and near users [10]. RIS can be used for millimeter wave communications [10, 11]. RIS allows to increase data rates in hybrid Radio Frequency (RF) Free Space Optical (FSO) systems when one hop uses RF communications and the second one is based on FSO [12]. In practical systems, RIS can be deployed with finite phase shifts leading to non perfect RIS [13]. The asymptotic outage probability of wireless communications using RIS was derived in [14, 15]. RIS using unnamed aerial vehicle has been suggested in [16]. RIS with artificial intelligence algorithms have been discussed in [1, 17]. RIS with phase shifts optimized using machine learning was studied in [18]. RIS with transmission probability optimization was considered in [19]. RIS with imperfect channel estimation was studied in [20, 21].

The contributions of the paper are:

- We analyze and optimize the throughput at the packet level while previous studies deal with symbol or bit error probability [9].
- We maximize the total throughput of NOMA using RIS. We optimize power allocation coefficients to near and far users as well as the number of reflectors per user. Power allocation and number of reflectors optimization has not been yet proposed in the literature.

The paper contains six sections. Section 2 presents the system model. Section 3 analyze and optimize the throughput. Section 4 extends the results to mutliple users NOMA. Section 5 provides theoretical and simulation results. Finally, Sect. 6 concludes the paper.

2 System Model

When RIS is used, the phase shift of a given reflector dedicated to kth user is optimized so that all reflections have the same phase. Different sets of reflectors are dedicated to the different users. The receiver output at kth user is similar to that of a Maximum Ratio Combiner (MRC) [2]. The system model is shown in Fig. 1. It contains a Base Station (BS) and two NOMA users U_1 and U_2. U_1 is the near user while U_2 is the far user. We denote by $\sqrt{\alpha}h_k$ the channel coefficient between BS and the kth reflecting meta-surface of RIS, $\alpha = \frac{1}{d^\beta}$ is the average power of channel coefficient, d is the distance between BS and RIS, β is the path loss exponent, h_k is a zero mean complex Gaussian random variable (r.v.) with variance one, i.e. $h_k \sim CN(0,1)$. We denote by $h_k = a_k e^{-j\theta_k}$ where $a_k = |h_k|$ the absolute value of h_k and θ_k is the phase of h_k. For

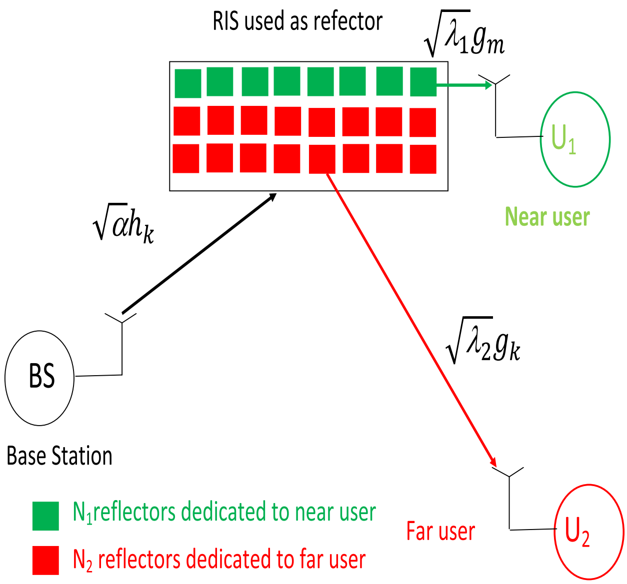

Fig. 1 NOMA using Reconfigurable Intelligent Surfaces (RIS)

Rayleigh channels, a_k is Rayleigh distributed with mean $E(a_k) = \frac{\sqrt{\pi}}{2}$ and second order moment $E(a_k^2) = 1$ where $E(X)$ is the expectation of X. Let $\sqrt{\lambda_i}g_k$ be the channel coefficient between kth reflecting meta-surface of RIS and user U_i where $\lambda_i = \frac{1}{d_i^{\beta}}$ is the average power of channel coefficient and d_i is the distance between RIS and U_i. $g_k = b_k e^{-j\psi_k} \sim CN(0,1)$, $b_k = |g_k|$ the absolute value of g_k and ψ_k is the phase of g_k. For Rayleigh channels, b_k is Rayleigh distributed with mean $E(b_k) = \frac{\sqrt{\pi}}{2}$ and second order moment $E(b_k^2) = 1$. We assume a Rayleigh block fading channel where channel coefficients h_k and g_k remain constant during packet duration.

It is assumed that RIS adjusts the phases Φ_k induced by the kth reflecting meta-surface such that

$$\Phi_k = \theta_k + \psi_k. \tag{1}$$

RIS assume a perfect knowledge of channel coefficient phases θ_k and ψ_k. As shown in Fig. 1, N_1 reflectors are dedicated to user U_1 while N_2 reflectors are dedicated to user U_2. Let $N = N_1 + N_2$ be the total number of available reflectors. Let I_1 and I_2 be the set of reflector indexes dedicated to U_1 and U_2. The number of reflectors in set I_i is $|I_i| = N_i$ where $|x|$ is the cardinality of set x. The received signals at U_1 and U_2 are equal to

$$y_1 = s\sqrt{2E_s\alpha\lambda_1}\sum_{k\in I_1} h_k g_k e^{j\Phi_k} + n_1, \tag{2}$$

$$y_2 = s\sqrt{2E_s\alpha\lambda_2}\sum_{k\in I_2} h_k g_k e^{j\Phi_k} + n_2, \tag{3}$$

where E_s is the transmitted energy per symbol of S, s is the transmitted symbol and n_i is a Gaussian noise with variance N_0.

The BS sends a combination of two symbols s_1 and s_2 dedicated to near and far users :

$$s = \sqrt{p_1}s_1 + \sqrt{p_2}s_2, \tag{4}$$

where p_i is the power allocation coefficient to user U_i such that $p_1 + p_2 = 1$. More power is allocated to far user U_2: $0 < p_1 < p_2 < 1$.

Using (1–3) and the expression of $h_k = a_k e^{-j\theta_k}$ and $g_k = b_k e^{-j\psi_k}$, the received signals at U_1 and U_2 are given by [2]

$$y_1 = s\sqrt{2E_s\alpha\lambda_1}\sum_{k\in I_1} a_k e^{-j\theta_k} b_k e^{-j\psi_k} e^{j\Phi_k} + n_1,$$

$$y_2 = s\sqrt{2E_s\alpha\lambda_2}\sum_{k\in I_2} a_k e^{-j\theta_k} b_k e^{-j\psi_k} e^{j\Phi_k} e^{j\Phi_k} + n_2,$$

Since $\Phi_k = \psi_k + \Phi_k$ (1), we obtain

$$y_1 = s\sqrt{2E_s\alpha\lambda_1}\sum_{k\in I_1} a_k b_k + n_1, \tag{5}$$

$$y_2 = s\sqrt{2E_s\alpha\lambda_2}\sum_{k\in I_2} a_k b_k + n_2, \tag{6}$$

Therefore, we can write

$$y_1 = \sqrt{X_1}s + n_1, \tag{7}$$

$$y_2 = \sqrt{X_2}s + n_2, \tag{8}$$

where

$$X_1 = 2E_s\alpha\lambda_1 A_1^2, \tag{9}$$

$$X_2 = 2E_s\alpha\lambda_2 A_2^2, \tag{10}$$

$$A_1 = \sum_{k\in I_1} a_k b_k, \tag{11}$$

and

$$A_2 = \sum_{k\in I_2} a_k b_k \tag{12}$$

Using (4-6), we obtain

$$y_1 = \sqrt{X_1}[\sqrt{p_1}s_1 + \sqrt{p_2}s_2] + n_1, \tag{13}$$

$$y_2 = \sqrt{X_2}[\sqrt{p_1}s_1 + \sqrt{p_2}s_2] + n_2. \tag{14}$$

3 Throughput Analysis and Optimization

In (14), the second term is the useful signal containing the symbol to be detected. The first term is the interference while last term is the noise. Therefore, far user U_2 detects its symbol s_2 with Signal to Interference plus Noise Ratio (SINR) [9]:

$$\Gamma_2 = \frac{p_2 X_2}{p_1 X_2 + N_0}. \tag{15}$$

During the first detection at near user, the first term of (13) is the interference from its own signal. The second term is the useful term of far user to be detected and the last one is noise. Therefore, near user U_1 detects first s_2 since $p_2 > p_1$ with SINR [9]

$$\Gamma_{1\to 2} = \frac{p_2 X_1}{p_1 X_1 + N_0}. \tag{16}$$

Then, near user removes the signal of U_2 (the second term in (13)) and detects its own symbol s_1 with SINR [9]

$$\Gamma_{1\to 1} = \frac{p_1 X_1}{N_0}. \tag{17}$$

The outage probability of user U_2 is equal to the probability that the SINR U_2 is lower than SINR threshold Γ_{th}:

$$P^{outage,2}(\Gamma_{th}) = P(\Gamma_2 \le \Gamma_{th}) = P(\frac{p_2 X_2}{p_1 X_2 + N_0} \le \Gamma_{th}) = P_{X_2}(\frac{N_0 \Gamma_{th}}{p_2 - p_1 \Gamma_{th}}) \tag{18}$$

where $P_{X_2}(x)$ is the Cumulative Distribution Function of X_2 equal to [22]

$$P_{X_2}(x) = P(X_2 \le x) = P(-\sqrt{\frac{x}{2E_s \alpha \lambda_2}} \le A_2 \le \sqrt{\frac{x}{2E_s \alpha \lambda_2}}) \tag{19}$$

Using the Central Limit Theorem (CLT), we can approximate A_i by a Gaussian r.v. with mean $m_{A_i} = \frac{N_i \pi}{4}$ and variance $\sigma^2_{A_i} = N_i(1 - \frac{\pi^2}{16})$ [2].

Therefore, we deduce

$$P_{X_2}(x) \simeq 0.5erfc\left(\frac{-\sqrt{\frac{N_0 x}{2E_s \alpha \lambda_2}} - m_{A_2}}{\sqrt{2}\sigma_{A_2}}\right) - 0.5erfc\left(\frac{\sqrt{\frac{N_0 x}{2E_s \alpha \lambda_2}} - m_{A_2}}{\sqrt{2}\sigma_{A_2}}\right) \tag{20}$$

There is no outage at U_1 when both SINRs $\Gamma_{1\to 1}$ and $\Gamma_{1\to 2}$ are greater than Γ_{th}

$$P^{outage,1}(\Gamma_{th}) = 1 - P(\Gamma_{1\to 1} > \Gamma_{th})P(\Gamma_{1\to 2} > \Gamma_{th})$$

$$= P_{X_1}(max[\frac{N_0 \Gamma_{th}}{p_2 - p_1 \Gamma_{th}}, \frac{N_0 \Gamma_{th}}{p_1}]), \tag{21}$$

where $P_{X_1}(x)$ is the CDF of X_1 expressed similarly to that of X_2 [22]:

$$P_{X_1}(x) \simeq 0.5erfc\left(\frac{-\sqrt{\frac{N_0 x}{2E_s\alpha\lambda_1}} - m_{A_1}}{\sqrt{2}\sigma_{A_1}}\right) - 0.5erfc\left(\frac{\sqrt{\frac{N_0 x}{2E_s\alpha\lambda_1}} - m_{A_1}}{\sqrt{2}\sigma_{A_1}}\right) \tag{22}$$

An upper bound of Packet Error Probability (PEP) at U_1 and U_2 are deduced from the outage probability [23]

$$PEP_1(p_1, p_2, N_1) < P^{outage,1}(T_0), \tag{23}$$

$$PEP_2(p_1, p_2, N_1) < P^{outage,2}(T_0), \tag{24}$$

where T_0 is a waterfall threshold defined as

$$T_0 = \int_0^{+\infty} PEP(x)dx, \tag{25}$$

where

$$PEP(x) = 1 - [1 - SEP(x)]^L, \tag{26}$$

L is the packet length in symbols and $SEP(x)$ is the Symbol Error Probability (SEP) for M-Quadrature Amplitude Modulation (QAM) [22]

$$SEP(x) = 2(1 - \frac{1}{\sqrt{M}})erfc(\sqrt{\frac{3x}{M-1}}) \tag{27}$$

The throughput at users U_1 and U_2 are computed as

$$Thr_1(p_1, p_2, N_1) = log_2(M)[1 - PEP_1(p_1, p_2, N_1)], \tag{28}$$

$$Thr_2(p_1, p_2, N_2) = log_2(M)[1 - PEP_2(p_1, p_2, N_2)]. \tag{29}$$

The total throughput is the sum of throughput at U_1 and U_2:

$$Thr(p_1, p_2, N_1, N_2) = Thr_1(p_1, p_2, N_1) + Thr_2(p_1, p_2, N_2). \tag{30}$$

In NOMA systems using RIS, more power $p_2 > p_1$ and more reflectors $N_2 > N_1$ should be allocated to far user U_2. Power allocation coefficients p_1, p_2 as well as number of reflectors N_1 and N_2 are optimized using the alternating maximization algorithm [24–26] to maximize the total throughput

$$Thr^{max} = \underset{0<p_1<p_2<1, N_1 \geq 1, N_2 = N - N_1}{Max}[Thr(p_1, p_2, N_1, N_2)]. \tag{31}$$

under constraint $p_1 + p_2 = 1$ and $N = N_1 + N_2$.

4 NOMA with Multiple Users Using RIS

The system model of NOMA with K users is shown in Fig. 2. N_i reflectors of RIS are dedicated to user U_i. The total number of reflectors is $N = \sum_{i=1} N_i$. I_i is the index of reflectors dedicated to user U_i. The number of reflector dedicated to U_i is $|I_i| = N_i$. When there are K users, the BS sends a linear combination of K symbols $s_i\, i = 1, \ldots, K$ to K NOMA users:

$$s = \sum_{i=1}^{K} \sqrt{p_i} s_i, \tag{32}$$

where $\sum_{i=1}^{K} p_i = 1$ and $0 < p_1 < p_2 < \cdots < p_K < 1$ are power allocation coefficients to users $U_1, U_2, \ldots U_K$.

The received signal at user U_i is expressed as

$$y_i = s\sqrt{KE_s \alpha \lambda_1} \sum_{k \in I_i} a_k b_k + n_i, \tag{33}$$

We deduce

$$y_i = s\sqrt{X_i} + n_i = \sum_{j=1}^{K} \sqrt{p_j} s_j \sqrt{X_i} + n_i, \tag{34}$$

where

$$X_i = KE_s \alpha \lambda_2 A_i^2, \tag{35}$$

$$A_i = \sum_{k \in I_i} a_k b_k, \tag{36}$$

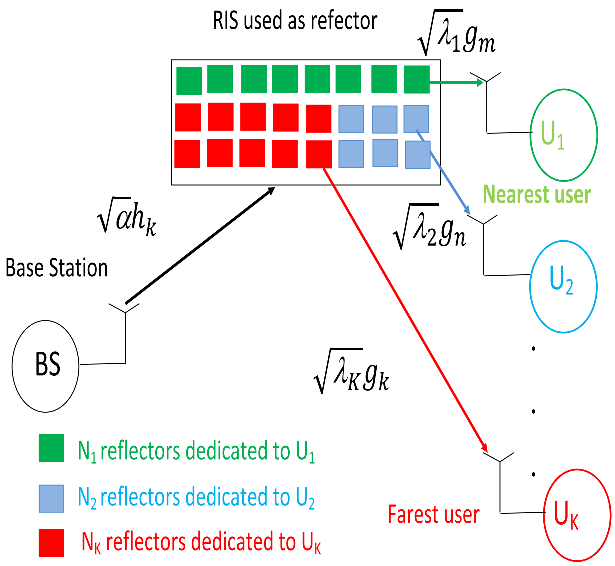

Fig. 2 NOMA with K users using Reconfigurable Intelligent Surfaces (RIS)

In (34), the Kth term is the useful signal to be detected by U_i during first detection and all other terms are interference. U_i detects first s_K since it is transmitted with a larger power $p_K > p_{K-1} > \cdots > p_i$. The SINR at U_i to detect s_K is equal to [9]

$$\Gamma_{i \to K} = \frac{X_i p_K}{N_0 + X_i \sum_{j=1}^{K-1} p_j} \tag{37}$$

Then, U_i removes the contribution of s_K (The Kth term in (34)) and detects s_{K-1} with SINR [9]

$$\Gamma_{i \to K-1} = \frac{X_i p_{K-1}}{N_0 + X_i \sum_{j=1}^{K-2} p_j} \tag{38}$$

Then, U_i removes the contribution of s_{K-1} (The (K-1)th term in (34)) and detects s_{K-2}. The process is repeated until U_i detects its symbol s_i. All terms with indexes $K, K-1, \dots, i+1$ will be removed during SIC iterations When detecting s_q, all terms of (34) with indexes $K, K-1, \dots, q+1$ will be removed. The useful term is the qth term in (34) and the other indexes $q-1, q-2, \dots, 1$ are interference from other users. The SINR at U_i to detect s_q, $i \le q \le K$, is equal to [9]

$$\Gamma_{i \to q} = \frac{X_i p_q}{N_0 + X_i \sum_{j=1}^{q-1} p_j}, i \le q \le K, \tag{39}$$

There is no outage at U_i if all SINRs $\Gamma_{i \to K}$, $\Gamma_{i \to K-1}$,..., $\Gamma_{i \to i}$ are larger than Γ_{th}. Therefore, the outage probability is equal to [9]

$$P^{outage,i}(\Gamma_{th}) = 1 - P(\Gamma_{i \to K} > \Gamma_{th}, \Gamma_{i \to K-1} > \Gamma_{th}, \dots, \Gamma_{i \to i} > \Gamma_{th})$$

$$P_{X_i}\left(\max_{i \le q \le K} \left(\frac{N_0 \Gamma_{th}}{p_q - \Gamma_{th} \sum_{j=1}^{q-1} p_j} \right) \right), \tag{40}$$

where [22]

$$P_{X_i}(x) \simeq 0.5 erfc\left(\frac{-\sqrt{\frac{N_0 x}{K E_s \alpha \lambda_i}} - m_{A_i}}{\sqrt{2}\sigma_{A_i}} \right) - 0.5 erfc\left(\frac{\sqrt{\frac{N_0 x}{K E_s \alpha \lambda_i}} - m_{A_i}}{\sqrt{2}\sigma_{A_i}} \right) \tag{41}$$

An upper bound of PEP at user U_i is deduced from the outage probability [23]

$$PEP_i(p_1, p_2, \dots, p_K, N_i) < P^{outage,i}(T_0), \tag{42}$$

where T_0 is a waterfall threshold defined in (25).

The throughput at user U_i are computed as

$$Thr_i(p_1, p_2, \dots, p_K, N_i) = log_2(M)[1 - PEP_1(p_1, p_2, \dots, p_K, N_i)], \tag{43}$$

The total throughput is the sum of throughput at all K users:

$$Thr(p_1,p_2,\dots,p_K,N_1,N_2,\dots,N_K) = \sum_{i=1}^{K} Thr_i(p_1,p_2,\dots,p_K,N_i). \quad (44)$$

In this paper, we propose to optimize power allocation coefficients p_1, p_2, ..., p_K as well as number of reflectors N_1, N_2, ..., N_K using the alternating maximization algorithm [24] to maximize the total throughput:

$$Thr^{max} = \underset{0<p_1<p_2<\cdots<p_K<1, N_i \geq 1}{Max}[Thr(p_1,p_2,\dots,p_K,N_1,N_2,\dots,N_K)]. \quad (45)$$

under constraint $\sum_{i=1}^{K} p_i = 1$ and $N = \sum_{i=1}^{K} N_i$.

5 Theoretical and Simulation Results

We have plotted theoretical PEP and throughput of NOMA with and without RIS. The average power of channel coefficient between nodes X and Y as $\frac{1}{d^\beta}$ where $\beta = 3$ is the path loss exponent and d is the distance between node X and Y. We have simulated packet containing 300 symbols and a packet is declared to be corrected only when all its symbols are correct. The Packet Error Rate (PER) measured during simulation is the percentage of erroneous packets. We did simulations until 200 packets are erroneously received. The distance between BS and RIS is $d = 1$. The distance between RIS and users U_1, U_2 and U_3 are $d_1 = 1$, $d_2 = 1.1$, $d_3 = 1.3$. These are normalized distances $d_i = \frac{d_i^{effective}}{d_0}$ where $d_i^{effective}$ is the effective distance between RIS and U_i in meters and d_0 is a reference distance.

Figures 3 and 4 show the PEP at far and near user for 16-QAM modulation and when there are $K = 2$ users and $N_1 = N_2 = 16, 32, 64, 128$. Power allocation coefficients are $p_1 = 1 - p_2 = 0.4$. As the number of reflectors is increases, as the PEP decreases. In fact, the signal at U_i can be viewed as the output of a Maximum Ratio Combination (MRC) of N_i signals [2]. We notice that the PEP of NOMA using RIS is lower than that of conventional NOMA without RIS.

Figures 5 and 6 show the average throughput at far and near users for 16-QAM modulation and when there are $K = 2$ users and $N_1 = N_2 = 16, 32, 64, 128$. We observe that the throughput increases as the number of reflectors is increased : $N_1 = N_2 = 16, 32, 64, 128$. When NOMA is employed with RIS, the throughput at far and near users is better than conventional NOMA without RIS.

Figures 7 and 8 show the total throughput for 16QAM modulation and when there are $K = 2$ users for 16QAM modulation. We observe that the throughput of NOMA using RIS is better than that of conventional NOMA. Besides, the throughput improved as the number of reflectors is increased $N_1 = N_2 = 16, 32, 64, 128$. In Fig. 7, power allocation coefficients are $p_1 = 1 - p_2 = 0.4$ and the same number of reflectors were dedicated to near and far users : $N_1 = N_2$. In Fig. 8, we have compared the total throughput when $p_1 = 1 - p_2 = 0.4$ to Optimal Power Allocation (OPA). We also considered a total number of reflectors $N = N_1 + N_2 = 32$. By optimizing both power allocation coefficients as well as the number of reflectors, we obtained a larger throughput than $N_1 = N_2 = 16$ where the same number of reflectors was dedicated to far and near users with $p_1 = 1 - p_2 = 0.4$. By optimizing power allocation coefficients and number of reflectors, we obtained up to 4 dB gain with respect to $N_1 = N_2 = 16$ and $p_1 = 1 - p_2 = 0.4$.

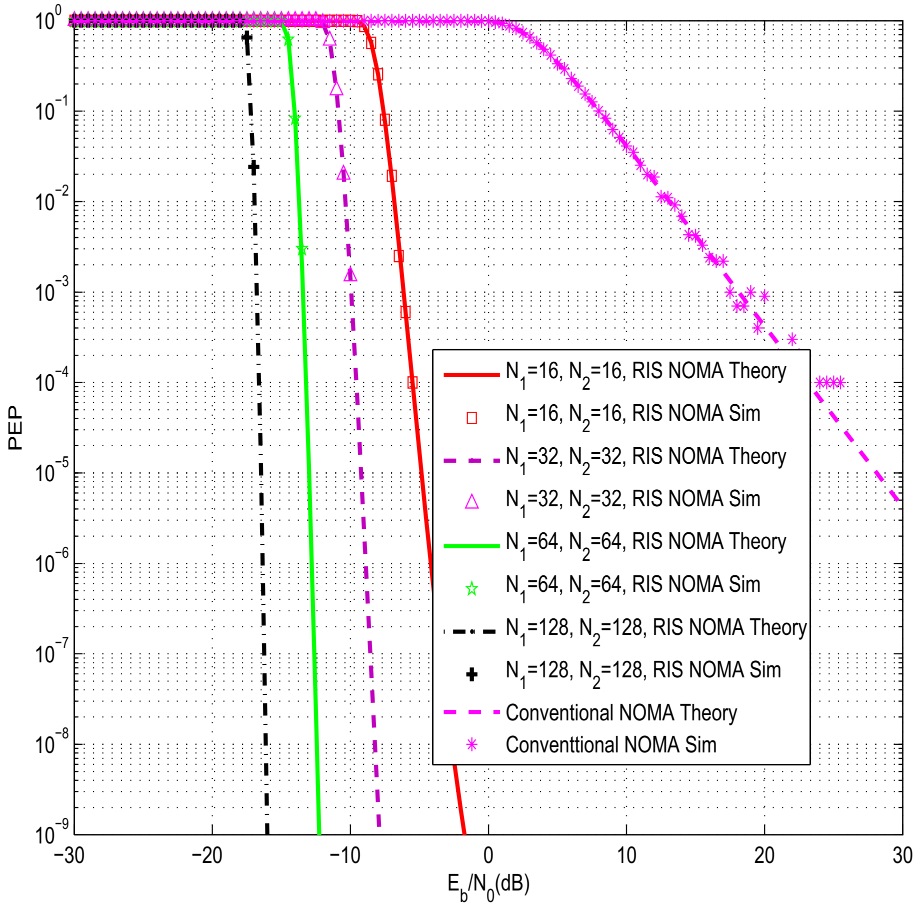

Fig. 3 PEP at far user

Figures 9 and 10 show the total throughput for 16QAM modulation and when there are $K = 3$ users for 16QAM modulation. We observe that the throughput of NOMA using RIS is better than that of conventional NOMA. Besides, the throughput improved as the number of reflectors is increased $N_1 = N_2 = N_3 = 16, 32, 64$. In Fig. 7, power allocation coefficients are $p_1 = 0.2, p_2 = 0.3, p_3 = 0.5$ and the same number of reflectors were dedicated to the three users : $N_1 = N_2 = N_3$. In Fig. 8, we have compared the total throughput when $p_1 = 0.2, p_2 = 0.3, p_3 = 0.5$ to OPA. We also considered a total number of reflectors $N = N_1 + N_2 + N_3 = 48$. The number of reflectors of RIS is 48. An uniform allocation consists to use $N_1 = N_2 = N_3 = 16$ reflectors for each user. In this paper, we optimize the number of reflectors per user by allocating more reflectors to weak users in order to maximize the total throughput. By optimizing both power allocation coefficients as well as the number of reflectors, we obtained a larger throughput than $N_1 = N_2 = N_3 = 16$ where the same number of reflectors was dedicated to all three users with $p_1 = 0.2, p_2 = 0.3, p_3 = 0.5$. By optimizing power allocation coefficients and

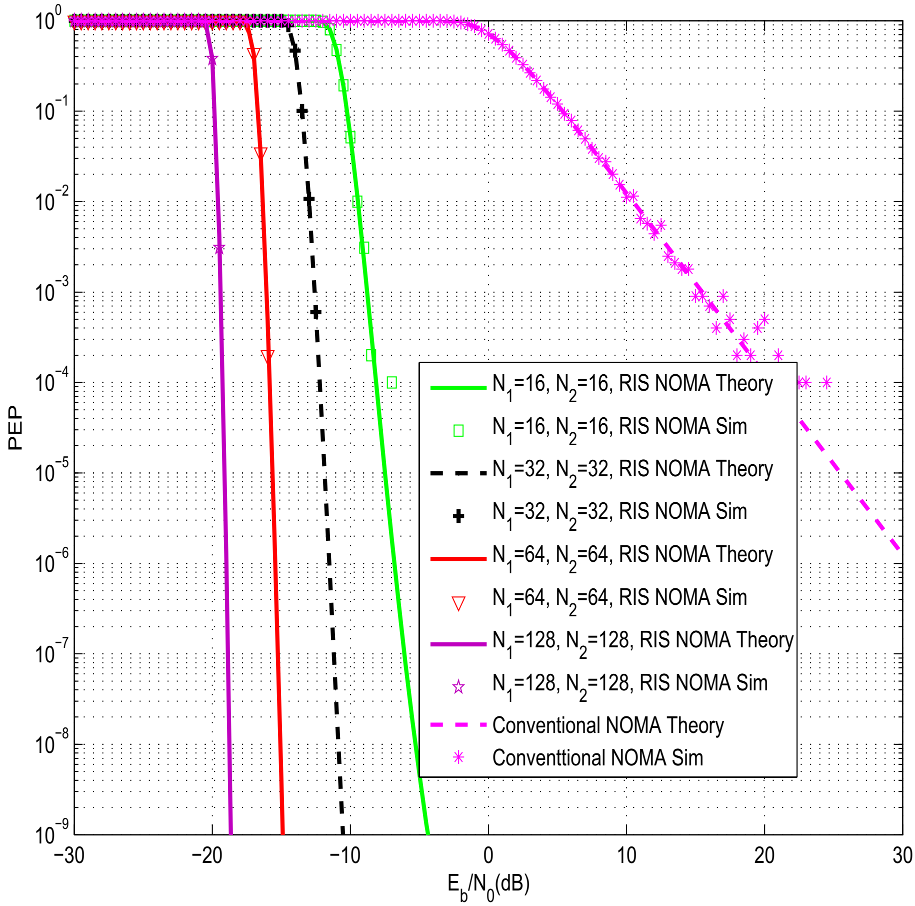

Fig. 4 PEP at near user

number of reflectors, we obtained up to 7 dB gain with respect to $N_1 = N_2 = N_3 = 16$ and $p_1 = 0.2, p_2 = 0.3, p_3 = 0.5$.

6 Conclusions

In this paper, we analyzed and optimized the throughput of Non Orthogonal Multiple Access (NOMA) using Reconfigurable Intelligent Surfaces (RIS). We optimized both power allocation coefficients as well as the number of reflectors per user to maximize the total throughput. We have shown that NOMA using RIS offers a higher throughput than conventional NOMA without RIS. By optimizing power allocation coefficients and number of reflector per user, we obtained a larger total throughput than fixed power allocation and the same number of reflectors per user.

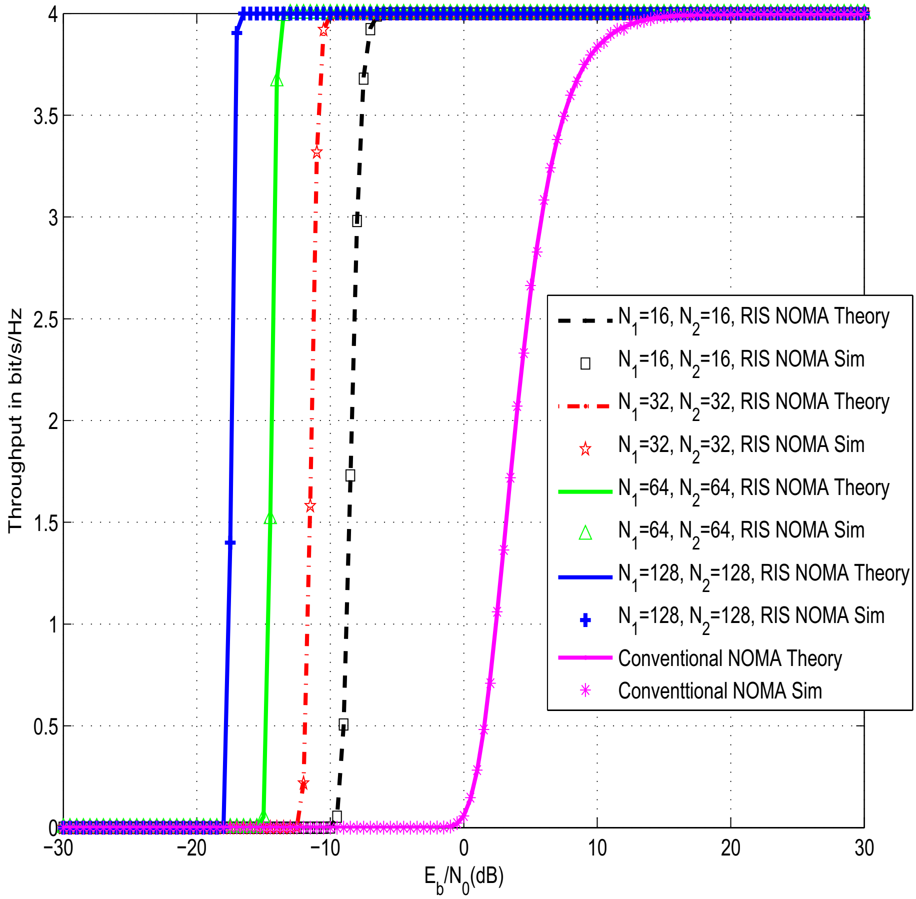

Fig. 5 Throughput at far user

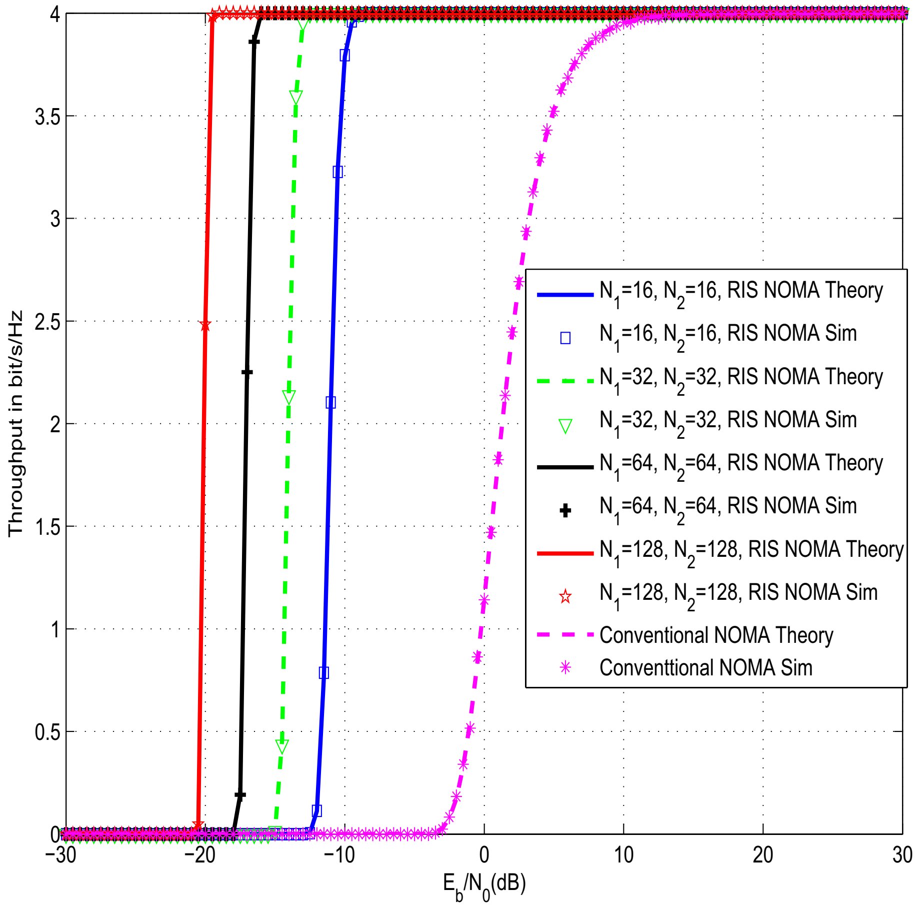

Fig. 6 Throughput at near user

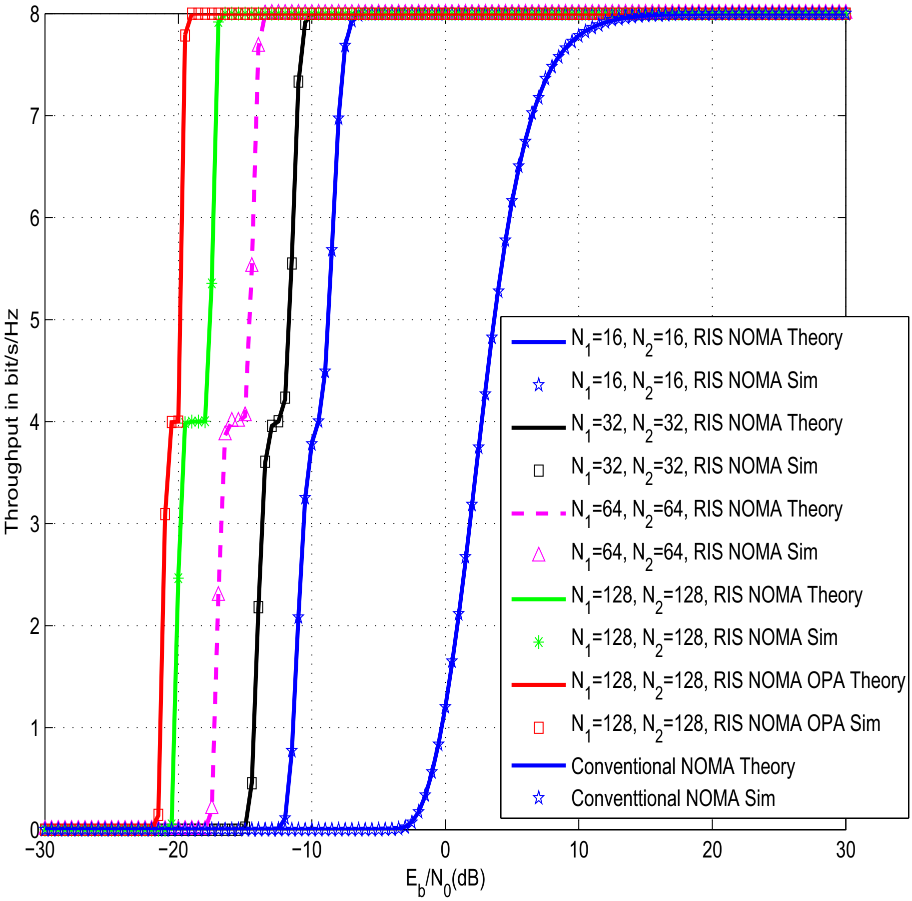

Fig. 7 Total throughput in the presence of two users

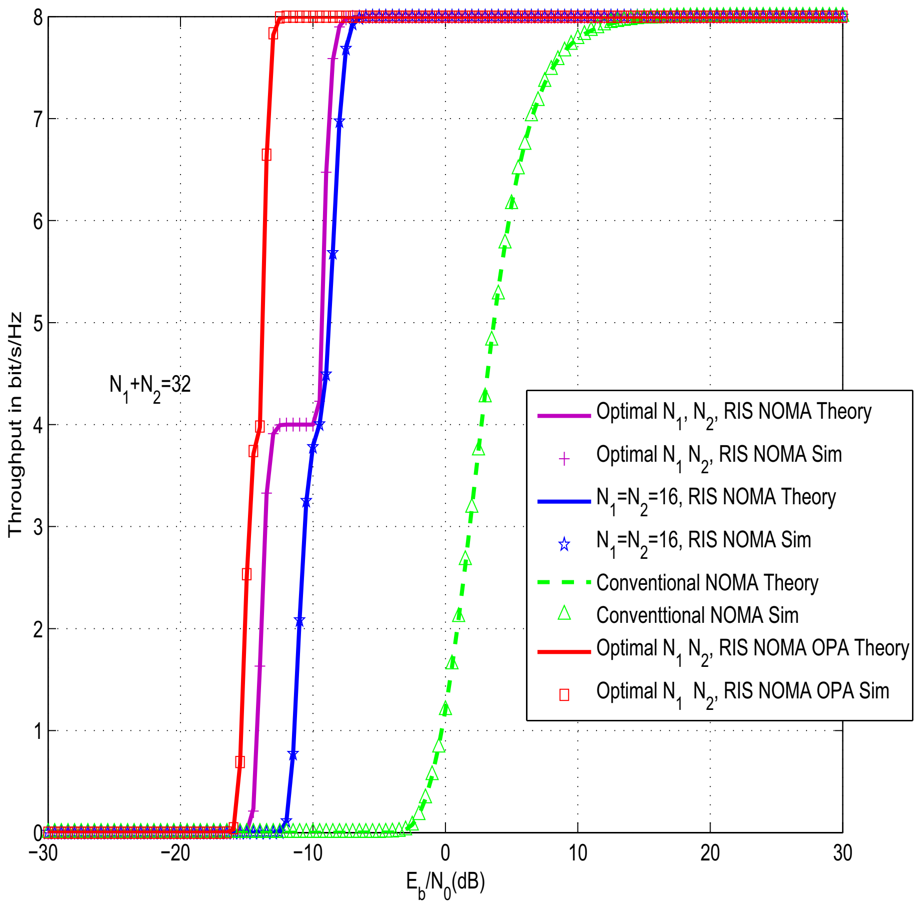

Fig. 8 Total throughput in the presence of two users with optimal number of reflectors and optimal power allocation

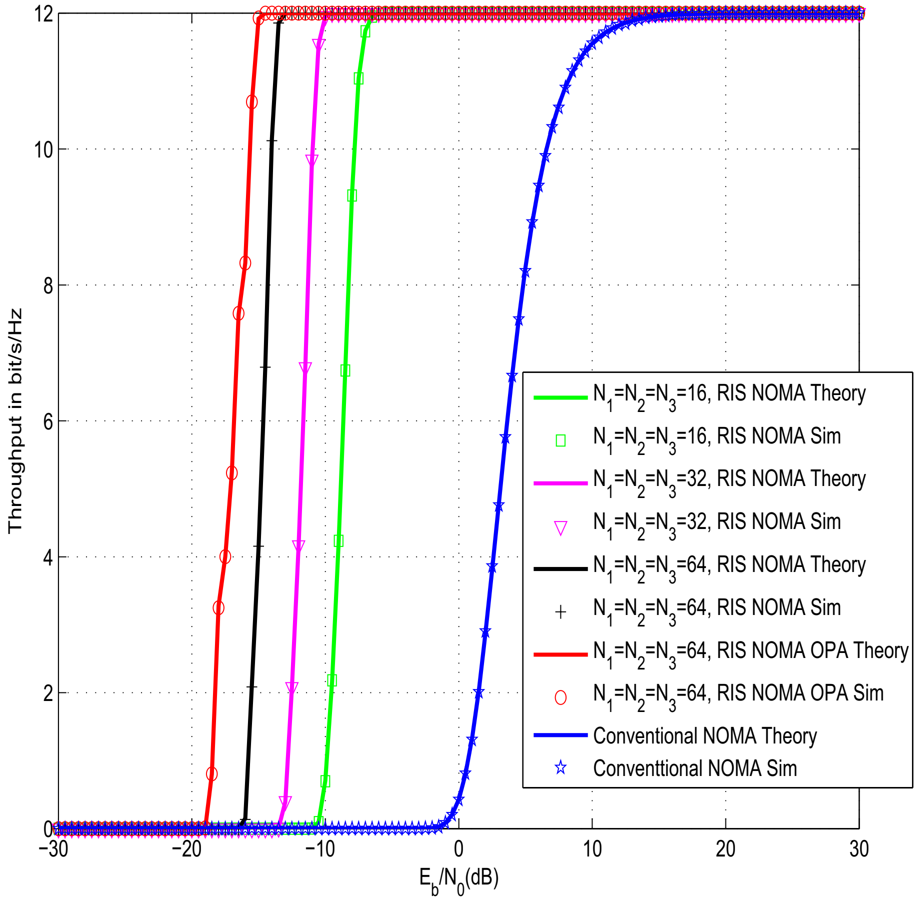

Fig. 9 Total throughput in the presence of three users

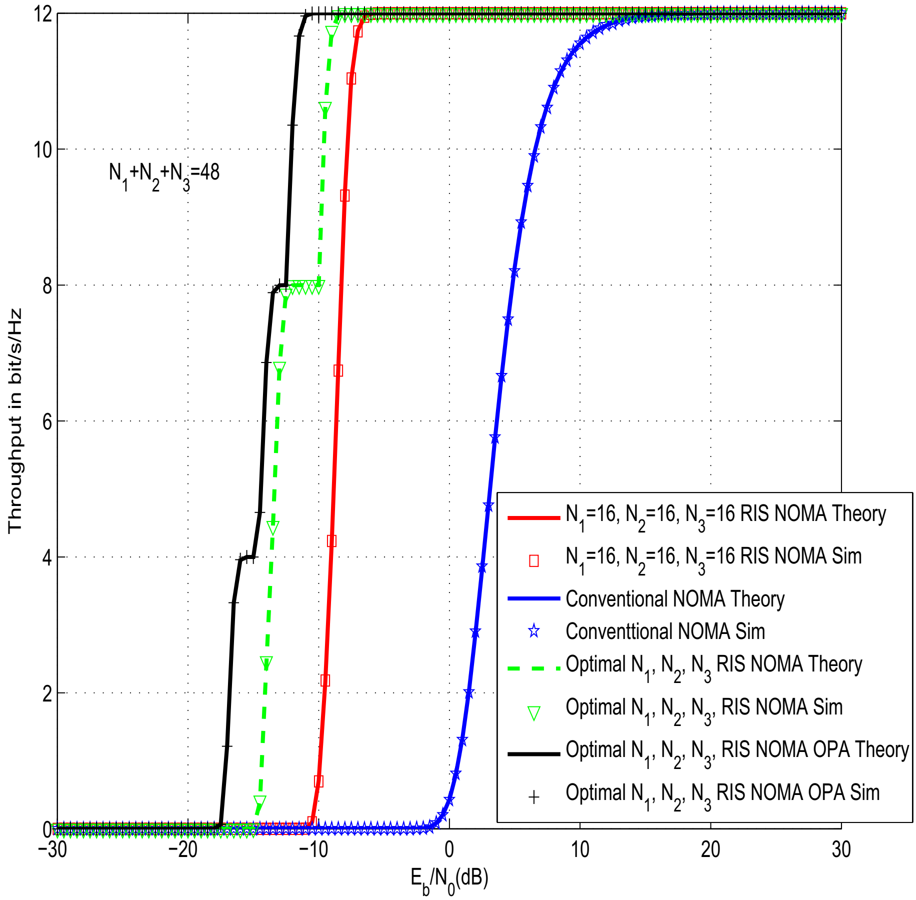

Fig. 10 Total throughput in the presence of three users with optimal number of reflectors and optimal power allocation

Author Contributions The paper is the contribution of Prof. Ghassan Alnwaimi and Prof. Hatem Boujemaa.

Funding This publication was not supportedThere is no conflict of interest for this paper.

Availability of data and material (data transparency) Data and material are not available.

References

1. Dai, L., Wang, B., Wang, M., Yang, X., Tan, J., Bi, S., et al. (2020). Reconfigurable intelligent surface-based wireless communications: Antenna design, prototyping, and experimental results. *IEEE Access, 8,* 45913–45923.
2. Basar, E., Di Renzo, M., De Rosny, J., Debbah, M., Alouini, M.-S., & Zhang, R. (2019). Wireless communications through reconfigurable intelligent surfaces. *IEEE Access, 7,* 116753–116773.
3. Zhang, H., Di, B., Song, L., & Han, Z. (2020). Reconfigurable intelligent surfaces assisted communications with limited phase shifts: How many phase shifts are enough? *IEEE Transactions on Vehicular Technology, 69*(4), 4498–4502.

4. Di Renzo, M. 6G wireless: Wireless networks empowered by reconfigurable intelligent surfaces. In *2019 25th Asia-Pacific conference on communications (APCC)*.
5. Wu, Q., & Zhang, R. (2020). Towards smart and reconfigurable environment: Intelligent reflecting surface aided wireless network. *IEEE Communications Magazine, 58*(1), 106–112.
6. Huang, C., Zappone, A., Alexandropoulos, G. C., Debbah, M., & Yuen, C. (2019). Reconfigurable intelligent surfaces for energy efficiency in wireless communication. *IEEE Transactions on Wireless Communications, 18*(8), 4157–4170.
7. Alexandropoulos GC, Vlachos E (2020) A hardware architecture for reconfigurable intelligent surfaces with minimal active elements for explicit channel estimation. In *ICASSP 2020 - 2020 IEEE international conference on acoustics, speech and signal processing (ICASSP).*
8. Guo, H., Liang, Y.-C., Chen, J., & Larsson, E. G. (2020). Weighted sum-rate maximization for reconfigurable intelligent surface aided wireless networks. *IEEE Transactions on Wireless Communications, 19,* 3064–3076.
9. Thirumavalavan, V. C., Jayaraman, T. S. (2020). BER analysis of reconfigurable intelligent surface assisted downlink power domain NOMA system. In *2020 international conference on communication systems and networks (COMSNETS).*
10. Pradhan, C., Li, A., Song, L., Vucetic, B., & Li, Y. (2020). Hybrid precoding design for reconfigurable intelligent surface aided mmWave communication systems. *IEEE Wireless Communications Letters, 9,* 1041–1045.
11. Ying, K., Gao, Z., Lyu, S., Wu, Y., Wang, H., & Alouini, M.-S. (2020). GMD-based hybrid beamforming for large reconfigurable intelligent surface assisted millimeter-wave massive MIMO. *IEEE Access, 8,* 19530–19539.
12. Yang, L., Guo, W., & Ansari, I. S. (2020). Mixed dual-hop FSO-RF communication systems through reconfigurable intelligent surface. *IEEE Communications Letters, 24,* 1558–1562.
13. Di, B., Zhang, H., Li, L., Song, L., Li, Y., & Han, Z. (2020). Practical hybrid beamforming with finite-resolution phase shifters for reconfigurable intelligent surface based multi-user communications. *IEEE Transactions on Vehicular Technology, 69*(4), 4565–4570.
14. Nadeem, Q.-U.-A., Kammoun, A., Chaaban, A., Debbah, M., & Alouini, M.-S. (2020). Asymptotic max-min SINR analysis of reconfigurable intelligent surface assisted MISO systems. *IEEE Transactions on Wireless Communications, 19,* 7748–7764.
15. Zhao, W., Wang, G., Atapattu, S., Tsiftsis, T. A., & Tellambura, C. (2020). Is backscatter link stronger than direct link in reconfigurable intelligent surface-assisted system? *IEEE Communications Letters, 24,* 1342–1346.
16. Li, S., Duo, B., Yuan, X., Liang, Y.-C., & Di Renzo, M. (2020). Reconfigurable intelligent surface assisted UAV communication: Joint trajectory design and passive beamforming. *IEEE Wireless Communications Letters, 9,* 716–720.
17. Huang, C., Alexandropoulos, G. C., Yuen, C., & Debbah, M. (2019). Indoor signal focusing with deep learning designed reconfigurable intelligent surfaces. In *2019 IEEE 20th international workshop on signal processing advances in wireless communications (SPAWC).*
18. Jiang, T., Cheng, H. V., & Yu, W. (2021). Learning to reflect and to beamform for intelligent reflecting surface with implicit channel estimation. *IEEE Journal on Selected Areas in Communications, 39*(7), 1931–1945.
19. Kong, J., Dagefu, F. T. , Choi, J., & Spasojevic, P. (2021). Intelligent reflecting surface assisted covert communication with transmission probability optimization. *IEEE Wireless Communications Letters*.
20. Dang, J., Zhang, Z., & Wu, L. (2020). Joint beamforming for intelligent reflecting surface aided wireless communication using statistical CSI. *China Communications, 17*(8), 147–157.
21. Zhao, M.-M., Wu, Q., Zhao, M.-J., & Zhang, R. (2021). Exploiting amplitude control in intelligent reflecting surface aided wireless communication with imperfect CSI. *IEEE Transactions on Communications, 69*(6), 4216–4231.
22. Proakis, J. (2007). *Digital Communications*, Mac Graw-Hill, 5th edition.
23. Xi, Y., Burr, A., Wei, J. B., & Grace, D. (2011). A general upper bound to evaluate packet error rate over quasi-static fading channels. *IEEE Transactions on Wireless Communications, 10*(5), 1373–1377.
24. Naiss, I., Permuter, H. H. Alternating maximization procedure for finding the global maximum of directed information. In *2010 IEEE 26-th convention of electrical and electronics engineers in Israel*.
25. Basar, E. (2020). Reconfigurable intelligent surface-based index modulation: A new beyond MIMO paradigm for 6G. *IEEE Transactions on Communications, 68,* 3187–3196.

26. Hua, S., Shi, Y. (2019). Reconfigurable intelligent surface for green edge inference in machine learning. In *2019 IEEE Globecom Workshops (GC Wkshps)*.

Ghassan Alnwaimi (M'14) received the B.Sc. degree (first honor) in electronics and communication engineering from King Abdulaziz University, Jeddah, Saudi Arabia, the M.Sc. degree (with distinction) in mobile and satellite communications from the University of Surrey, Guildford, U.K., and the Ph.D. degree from the Institute for Communication Systems (formerly Centre for Communication Systems Research), University of Surrey, in 2014. He is an Associate Professor with the Department of Electrical and Computer Engineering, King Abdulaziz University. His research interests include the design of cognitive radio systems, self-organization networks, spectrum sensing, spectrum management, dynamic spectrum access techniques, and interference management in femtocells and heterogeneous networks.

Hatem Boujemaa (M'02) was born in Tunis, Tunisia. He received the Engineer's Diploma from " Ecole Polytechnique de Tunis", in 1997, the MSC in digital communications from "Telecom Paris Tech", in 1998 and the Ph. D. degree in electronics and communications from the same university in 2001. From October 1998 to September 2001, he prepared his Ph. D. degree at France Telecom R&D, Issy-les-Moulineaux, France. During this period, he participated in the RNRT project AUBE. From October 2001 to January 2002, he joined "Ecole Supérieure d'Electricité", Gif-sur-Yvette, France, and worked on mobile localization for RNRT project LUTECE. In February 2002, he joined SUPCOM where he is a Professor. His research activities are in the field of digital communications, DS-CDMA, OFDM and MC-CDMA systems, HARQ protocols, Cooperative Communications, Cognitive radio networks, Scheduling, Synchronization, Network planning, Information Theory, Equalization and Antenna Processing.